

# Computer simulation of coherent interaction of charged particles and photons with crystalline solids at high energies

Armen Apyan\*

*Northwestern University, Department of Physics and Astronomy, 2145 Sheridan Road, Evanston, IL 60208, USA*

Monte Carlo simulation code has been developed and tested for studying the passage of charged particle beams and radiation through the crystalline matter at energies from tens of MeV up to hundreds of GeV. The developed Monte Carlo code simulates electron, positron and photon shower in single crystals and amorphous media. The Monte Carlo code tracks all the generations of charged particles and photons through the aligned crystal by taking into account the parameters of incoming beam, multiple scattering, energy loss, emission angles, transverse dimension of beams, and linear polarization of produced photons.

The simulation results are compared with the CERN-NA-59 experimental data. The realistic descriptions of the electron and photon beams and the physical processes within the silicon and germanium single crystals have been implemented.

PACS numbers: 41.60.-m, 25.20.Dc, 24.10.Lx, 87.18.Bb

Keywords: Monte Carlo simulations, Coherent Bremsstrahlung, Single Crystal, Electromagnetic shower

## I. INTRODUCTION

In the last decade, the electromagnetic interaction of charged particles and photons with crystalline and amorphous media are intensively investigated both theoretically and experimentally. Special attention was given to the investigation of interaction of charged particles and photons with crystalline media. An electron or photon impinging on a crystal will interact coherently with the atoms in aligned crystal axes or planes. If the Laue condition is satisfied, the coherent bremsstrahlung (CB) or coherent pair production (CPP) phenomena are manifested [1]. The essential characteristics of the phenomena are quasi-monochromatic spectrum, high intensity and linear polarization degree of radiation in coherent maximum. The intensity of the coherent bremsstrahlung in aligned crystals is few ten times greater than in amorphous media at the certain energy region. The same characteristics are seen in CPP by photons in the single crystals. The processes of CB and CPP in single crystals are well investigated and understood both theoretically [1] and experimentally [2, 3].

In this work we describe briefly the physical processes involved, the simulation model and the results of the Monte Carlo simulations for high energy particles traversing an aligned single crystals.

It is well known that the dominant energy loss mechanism for high energy electrons and positrons is the production of electromagnetic radiation, i.e. bremsstrahlung for motion through the matter. The high energy photons become absorbed mainly due to the  $e^+e^-$  pair production in a matter. This is true for crystals as well. In our simulations we ignored the processes such as Compton scattering, photoeffect, energy loss in ionization, nuclear processes due to smallness of their cross section and

negligible contribution in total cross section. Electron or photon beams penetrating the crystal will create an electromagnetic shower (EMS) via the CB, CPP or incoherent bremsstrahlung (ICB) and pair production (IPP) depending on the orientation of crystal axes and planes relative to incident particle momentum.

There are broad experimental and theoretical investigations devoted to the EMS development in various amorphous media and energies. Many general - purpose Monte Carlo simulation packages (see Ref. [4] and references cited therein) for transport of particles and radiation through the amorphous media are developed and have been successfully used in the last decades.

The electromagnetic interaction processes in aligned crystals are more complicated than in amorphous media. The cross section of interaction strongly depends on the crystal type, its orientations as well as on the energy, angular distribution and polarization of initial photon or electron beams.

The EMS in single crystals was mainly considered in channeling regime, when electrons and photons penetrate the crystal along a direction close to the one of main crystallographic axes [5, 6]. We consider EMS in single crystals oriented in CB mode. All the above mentioned peculiarities of coherent processes are carefully taken into account in Monte Carlo computer code.

## II. THEORETICAL BACKGROUND

Differential cross section of coherent radiation in a crystal is composed of two terms [1] coherent and incoherent bremsstrahlung

$$d\sigma = d\sigma_{inc} + d\sigma_{coh} \quad (1)$$

The first term corresponds to the incoherent cross section (including radiation in the field of the atomic nucleus and electrons) on  $N$  independent atoms. The sec-

---

\*E-mail address: aapyan@lotus.phys.northwestern.edu

and one corresponds to the coherent radiation cross section. Let us denote  $(E_0, \mathbf{P}_0)$ ,  $(E_1, \mathbf{P}_1)$  and  $(E_\gamma, \mathbf{P}_\gamma)$  as the energy and momentum of incoming, outgoing electrons and emitted photon, respectively. The initial beam orientation with respect to the crystal axes is defined by two angles in the following manner. The three chosen orthogonal axes of cubic crystal are  $[\mathbf{b}_1 \mathbf{b}_2 \mathbf{b}_3]$ . The initial beam orientation is defined by the angle  $\theta_0$  between the initial electron momentum  $\mathbf{P}_0$  and crystal axis  $\mathbf{b}_3$  and by the angle  $\psi_0$  between the electron momentum and crystal plane  $(\mathbf{b}_1 \mathbf{b}_3)$ . Let  $\theta$  and  $\varphi$  be the emitted photon polar and azimuthal angles with respect to the direction

of initial motion of the electron. Usually the polar angle is presented in the units of  $mc^2/E_{in}$ :

$$u = \frac{E_{in}}{mc^2}\theta \quad (2)$$

where  $E_{in}$  is the energy of initial particle,  $m$  is the electron rest mass and  $c$  is speed of light.

The angular-spectral distribution of CB (after integration with respect to exit angles of electrons) is given by the following expressions [1]:

$$d\sigma^3(x, \theta_0, \alpha_0, \xi, \varphi) = \frac{N\sigma_0}{2\pi} \frac{dx}{x} d\xi d\varphi I(x, \theta_0, \alpha_0, \xi, \varphi) \quad (3)$$

$$I(x, \theta_0, \alpha_0, \xi, \varphi) = \left[1 + (1-x)^2\right] \left(\Psi_1^{coh} + \Psi_1^{inc} + \Psi_1^{el}\right) - \frac{2}{3}(1-x) \left(\Psi_2^{coh} + \Psi_2^{inc} + \Psi_2^{el}\right) \quad (4)$$

where  $I(x, \theta_0, \alpha_0, \xi, \varphi)$  is the intensity of radiation,  $N$  is the number of atoms in a crystal,  $\sigma_0 = Z^2 r_0^2 \alpha$ ,  $Z$  is the atomic number of medium,  $r_0$  is the classical electron radius,  $\alpha$  is the fine structure constant,  $x = E_\gamma/E_0$  is the relative energy of emitted photon and  $\xi = 1/(1+u^2)$ .

The  $\psi_{1,2}^{coh}$  functions in equation Eq. 4 have the following structure [1]:

$$\begin{aligned} \Psi_1^{coh} &= 4 \sum_{\mathbf{g}} D_g g_\perp^2 \delta_D \left[ \frac{\delta}{\xi} - g_\parallel \right] \\ \Psi_2^{coh} &= 24 \sum_{\mathbf{g}} D_g \xi (1-\xi) g_\perp^2 \delta_D \left[ \frac{\delta}{\xi} - g_\parallel \right] \\ D_g &= \frac{(2\pi)^2 |S(\mathbf{g})|^2 [1-F(g)]^2}{\Delta N_0 g^4} \exp(-\bar{A}g^2) \end{aligned} \quad (5)$$

where  $\delta_D$  is Dirac's delta function,  $\mathbf{g}$  is the reciprocal lattice vector,  $\Delta$  is the volume of an elementary cell of a direct lattice,  $S(\mathbf{g})$  is the structure factor of the crystal,  $\bar{A}$  is the root mean square of thermal displacement amplitude of an atom from an equilibrium position. In our calculations we used Doyle-Turner parameterization [7] for the atomic formfactor  $F(g)$ . For a given orientation of the crystal, the longitudinal  $g_\parallel$  and transverse  $g_\perp$  component of  $\mathbf{g}$  with respect to the initial electron momentum  $\mathbf{P}_0$  are:

$$\begin{aligned} g_\parallel &= g_3 \cos \theta_0 + (g_1 \cos \alpha_0 + g_2 \sin \alpha_0) \sin \theta_0 \\ g_\perp^2 &= g^2 - g_\parallel^2 \end{aligned} \quad (6)$$

where  $g_1, g_2, g_3$  are the projections of  $\mathbf{g}$  on the crystal axes  $[b_1 b_2 b_3]$ . The  $\hbar\delta$  is a minimal value of the momentum transferred to medium along the direction of motion of primary particle:

$$\hbar\delta = \frac{\hbar E_\gamma m c^2}{2E_0 E_1} m c \quad (7)$$

where  $\hbar$  is the reduced Planck's constant.

The incoherent  $\psi_{1,2}^{inc}$  functions in equation Eq. 4 have the following structure [8]:

$$\begin{aligned} \Psi_1^{inc} &= 6 + 4\Gamma(\xi) \\ \Psi_2^{inc} &= 6 + 24\xi(1-\xi)\Gamma(\xi) \end{aligned} \quad (8)$$

where

$$\Gamma(\xi) = \ln \left( \frac{mc}{\hbar\delta} \right) - 2 - f(\zeta) + \mathfrak{F}(\hbar\delta/\xi) \quad (9)$$

is the general expression for  $\Gamma(\xi)$  for arbitrary screening. The quantity  $\mathfrak{F}(\hbar\delta/\xi)$  has the following form [8]:

$$\mathfrak{F}(\hbar\delta/\xi) = \int_{\hbar\delta/\xi}^{\infty} \left\{ 1 - \exp \left( -\frac{\bar{A}q^2}{\hbar^2} \right) \right\} \left\{ [1 - F(q)^2] - 1 \right\} \frac{(q^2 - (\hbar\delta)^2/\xi^2)}{q^3} dq \quad (10)$$

where  $q$  is the momentum transferred to the nucleus. The quantity  $f(\zeta)$  is the Coulomb correction:

$$f(\zeta) = \zeta^2 \sum_{n=1}^{\infty} \frac{1}{n(n^2 + \zeta^2)} \quad (11)$$

where  $\zeta = Z\alpha$ . The corrections due to contributions by

the atomic electrons, i.e. quantities  $\Psi_{1,2}^{el}$  were calculated by the theory given in [9].

The threefold differential cross section of CPP by photons in single crystals can be written in the following form [1]:

$$d\sigma^3(y, \theta_0, \alpha_0, \xi, \varphi) = \frac{N\sigma_0}{2\pi} dy d\xi d\varphi I(y, \theta_0, \alpha_0, \xi, \varphi) \quad (12)$$

$$I(y, \theta_0, \alpha_0, \xi, \varphi) = [y^2 + (1-y)^2] (\Psi_1^{coh} + \Psi_1^{inc} + \Psi_1^{el}) + \frac{2}{3} y(1-y) (\Psi_2^{coh} + \Psi_2^{inc} + \Psi_2^{el}) \quad (13)$$

Here we use the following notation. The  $(E_\gamma, \mathbf{P}_\gamma)$  are the initial photon energy and momentum and  $(E_+, \mathbf{P}_+)$ ,  $(E_-, \mathbf{P}_-)$  are the energy and momentum of produced positron and electron pair. The  $y = E_+/E_\gamma$  is the relative energy of produced positron,  $u = (E_+/mc^2)\theta_+$  and  $\theta_+$  is the angle between the positron and photon momenta. In case of CPP a minimal value of the momentum transferred to medium along the direction of motion of primary particle has the form:

$$\hbar\delta = \frac{\hbar E_\gamma mc^2}{2E_+ E_-} mc \quad (14)$$

The above described parameters are the same as for CB theory.

Computed differential cross sections of CB (Eq. 3 integrated over the emitted photon angles  $(\theta, \varphi)$ ) and CPP (Eq. 12 integrated over the production angles  $(\theta_\pm, \varphi_\pm)$  of  $e^+e^-$  pairs) are given in Fig. 1.

The top figure represents the spectral distribution of CB depending on the photon energy,  $x = E_\gamma/E_0$ , on the Si and Ge single crystals. For an  $E_0 = 178.2 GeV$  electron beam making an angle of  $\theta_0 = 30 mrad$  from the  $\langle 001 \rangle$  crystallographic axis and  $\psi_0 = 180 \mu rad$  from the (110) plane of Si crystal, the maximum peak intensity occurs in the vicinity of 100 GeV as seen in Fig. 1. The angle  $\psi_0 = 187 \mu rad$  was chosen for the corresponding spectral distribution in case of Ge crystal.

The differential cross sections of CPP in Si and Ge single crystals are given in the bottom of Fig. 1 depending on the energy of the  $e^+e^-$  pair component,  $y = E_\pm/E_\gamma$ . The total cross section of CPP has a maximum value for the chosen primary photon energy  $E_\gamma = 178.2 GeV$  and orientation angles  $\theta_0 = 30 mrad$  from the  $\langle 001 \rangle$  crystallographic axis and  $\psi_0 = 0.6 mrad$  from the (110) plane.

Particles could undergo transmission at small angles with respect to the crystal axes and planes due to angular divergence and multiple scattering during the EMS development in crystal. CB and CPP processes have strong

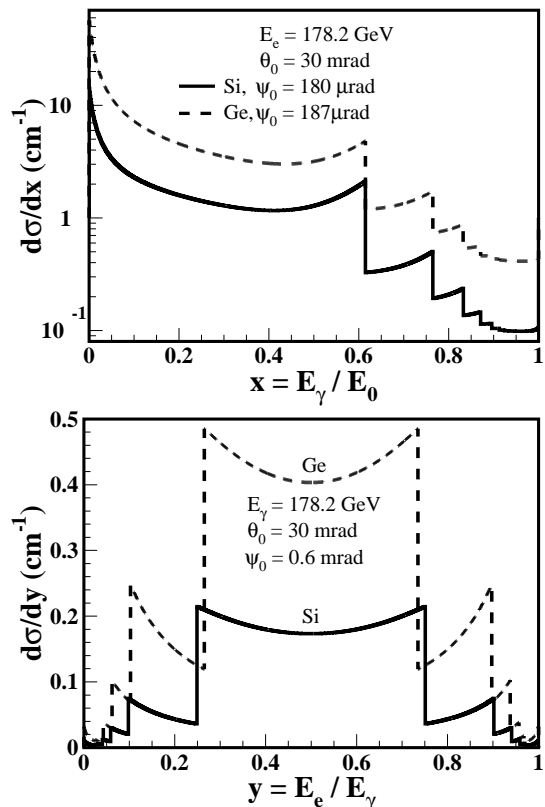


FIG. 1: Differential cross sections of CB (top) as a function of photon energy,  $x = E_\gamma/E_0$ , and CPP (bottom) as a function of the energy of the  $e^+e^-$  pair component,  $y = E_\pm/E_\gamma$  for Si (solid curves) and Ge (dashed curves) single crystals.

angular and energy dependences and the validity conditions of the Born approximation no longer hold at very high energies and small incidence angles with respect to the crystal axes and planes. The onset of this problem for the description of radiation emission and pair production has the characteristic angle  $\theta_v = U_0/mc^2$  [10],

where  $U_0$  is the plane potential well depth. The CB and CPP theory may be applied for the incidence angles with respect to the crystal axes/planes  $\theta_0 \gg \theta_v$ . The general theory of radiation and pair production is used [10, 11] for incident angles  $\theta_0 \sim \theta_v$  and  $\theta_0 < \theta_v$ .

### III. MONTE CARLO SIMULATIONS

#### A. General Considerations

Monte Carlo simulation technique of EMS development in oriented single crystals is based on the coherent radiation and coherent  $e^+e^-$  pair production processes at high energies. The program includes the formulae of coherent and quasiclassical theories for radiation and pair production. The program calculated the cross sections directly using the formulae of coherent effects (Eqs. 3 and 12). The quasiclassical theory was applied for calculating the cross sections in case of small incident angles with respect to the crystal axes or planes. Direct calculations by the formulae of this theory takes large computer time. Because the computer time needed to perform all the simulations is formidable, we used a data bank of pre-calculated cross sections of radiation and pair production to save the computer time. The data bank contains the total and differential cross sections on dependence of crystal type and its orientation, energy, horizontal and vertical angles and polarization. The cross sections for certain energy, angles, polarization were found by interpolation of the numerical values of cross sections stored in a data bank. The interpolated values of cross sections differ from calculated values  $\sim 2 - 3\%$ . We find that our approach yields very accurate numerical results for theory and a further saving of computer time.

#### B. Simulation model

The simulation model used in this work is based on random walk or particle history, where a history corresponds to following a particle from entering the medium, interacting and leaving it. Each particle history  $i$  can be represented by the array  $\mathbf{S}_j^i$  [12] denoting the state of particle before  $j$ th interaction:

$$\mathbf{S}_j^i = (\mathbf{r}_j^i, \boldsymbol{\Omega}_j^i, \boldsymbol{\eta}_j^i, E_j^i, q_j^i) \quad (15)$$

where  $\mathbf{r}_j^i, \boldsymbol{\Omega}_j^i, \boldsymbol{\eta}_j^i, E_j^i, q_j^i$  represent the electron or photon position, direction, polarization, energy and charge before each interaction act, respectively.

The initial particles, electrons or photons, generate two secondaries after each interaction. The initial electron loses energy via bremsstrahlung and produces secondary electron and bremsstrahlung photon. The electron can produce several photons during the traveling through matter. The number of produced photons depend on the thickness of the crystalline target and its orientation.

The initial photon is transformed into the  $e^+e^-$  pair after interaction. The simulation code calculates new state of particles and state of produced particles after each interaction act. A history is terminated when the particle energy drops below a low energy cut-off, or when particle moves outside to the target.

The similar simplified Monte Carlo simulation model was employed in [13, 14]. The simulation procedure has been improved by taking into account the peculiarities of the emission angles of photons and electrons in case of coherent effects (see Eq. 5). This improvement gives the possibility to use the code for simulation of production of collimated photon beams from thin crystals ( $\sim 20 - 100\mu m$ ) [15]. Polarization dependent cross sections and transverse dimensions of the particles beams are also implemented in the code.

### IV. SIMULATION RESULTS AND DISCUSSION

#### A. Comparison with experiment

A series of Monte Carlo simulations were performed for prediction of the results of CERN NA59 experiment. The goal of the experiment was the production of linearly polarized photon beams and conversion of the linear polarization into circular with the help of oriented single crystals [2, 3, 16, 17, 18].

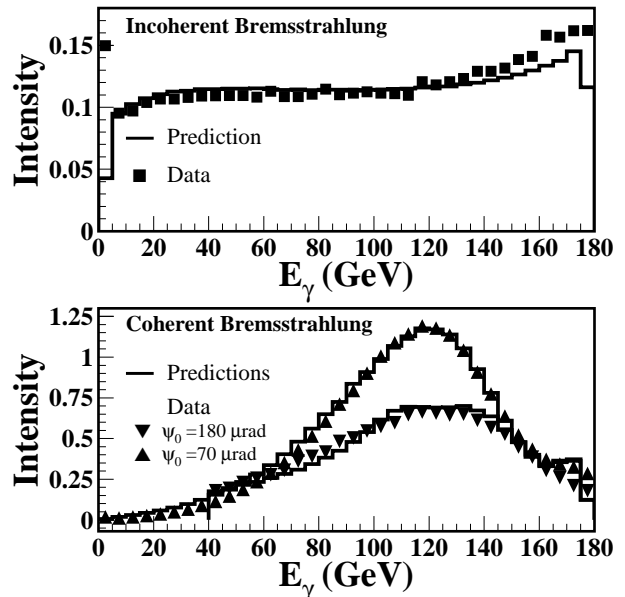


FIG. 2: Total energy radiated for incoherent (top) and coherent (bottom) bremsstrahlung radiation in 1.5 cm thick silicon crystal [3, 18]. The solid curves represent Monte Carlo simulation results. The experimental results are: (■) - for unaligned silicon crystal, (▲) -  $\psi_0 = 70\mu rad$ , (▼) -  $\psi_0 = 180\mu rad$ .

The comparison of Monte Carlo simulation data with experimental data are given in Fig. 2. The top figure represent the simulated and measured total radiated energy

TABLE I: Crystals and their orientations, radiation and absorption lengths used in the simulations.

Crystal	EMS	Orientation (mrad)	$L_R$ or $L_A$ (cm)
Si	Initiated by $e^-$	$\theta_0=30; \psi_0=0.180$	2.88 (9.36)
Si	Initiated by $\gamma$	$\theta_0=30; \psi_0=0.6$	5.45 (12.03)
Ge	Initiated by $e^-$	$\theta_0=30; \psi_0=0.187$	1.01 (2.30)
Ge	Initiated by $\gamma$	$\theta_0=30; \psi_0=0.6$	1.76 (2.96)

for 1.5 cm thick unaligned silicon crystal. The disoriented silicon crystal acts as an amorphous medium, hence we have incoherent bremsstrahlung spectra.

The bottom figure represents the simulated and measured CB spectra for the two orientations of silicon crystal with respect to incident electron beam. The electron beam was incident at an angle of  $\theta_0 = 5\text{mrad}$  to axis  $\langle 100 \rangle$  for both settings of silicon crystal. For the upper curve, the electron momentum makes an angle of  $\psi_0 = 70\mu\text{rad}$  with respect to the (110) plane and  $\psi_0 = 180\mu\text{rad}$  for lower curve.

The experimental data are taken from [3, 18]. The prominent agreement between the results of simulation and experimental data is seen. The described Monte Carlo simulation code allows prediction of the photon spectra, linear and circular polarizations, optimal orientation and thickness of used crystals.

## B. Electromagnetic shower

The developed code is capable to track the all generations or histories of electrons and photons in crystal. Thus, it can be used for simulation of EMS development in single crystals oriented in CB mode. We considered EMS initiated by the high energy electrons and photons in oriented silicon and germanium single crystals. The incident electron and photon beams parameters (energy, orientation angles, angular spread) are identical with those in NA59 experiment and discussed above (Section II and Fig. 1).

All calculations are carried out for the energy of initial particles (electrons or photons) of 178.2 GeV. The simulations takes into account the initial electron beam angular divergence in both horizontal ( $48\mu\text{rad}$ ) and vertical ( $33\mu\text{rad}$ ) planes. The types of single crystals and their orientations used in Monte Carlo simulations are presented in Table I. A low energy cut-off of 5 GeV was placed on the production of all secondary particles. In this study no distinction is made between electrons and positrons (later on simply electrons).

Important quantities in EMS development in matter are the radiation length ( $L_R$ ) for charged particles and absorption length ( $L_A$ ) for photons. There is a weak dependence of these quantities on particle energy in amorphous media. Practically  $L_R$  and  $L_A$  are constant for a given amorphous material. There is a strong dependence

of  $L_R$  and  $L_A$  on crystal type, its orientation, particle energy and polarization in case of oriented single crystals. The corresponding radiation and absorption lengths for aligned and unaligned crystals (in parenthesis) are given in Table I. One can see a large reduction of  $L_R$  and  $L_A$  in case of aligned crystals in comparison with amorphous media.

Fig. 3 and Fig. 4 represent the Monte Carlo simulation results of longitudinal EMS development in silicon and germanium single crystals in energy range  $5\text{ GeV} < E < 175\text{ GeV}$ . The energy carried by EMS is shown on the top figures in dependence on radiation and absorption lengths. The bottom figures show the dependence of number of particles on radiation and absorption lengths.

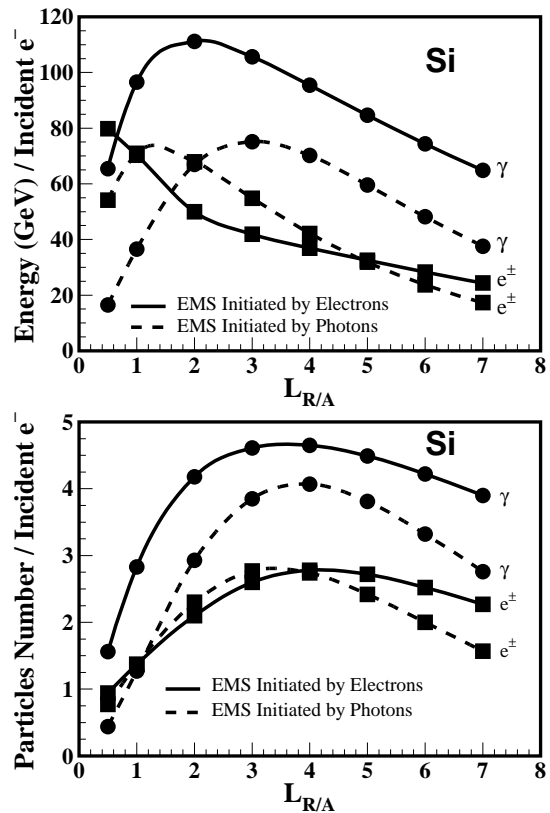


FIG. 3: The energy (top) and number of particles (bottom) of EMS as a function of thickness of an aligned silicon single crystal.  $L_{R/A}$  are the effective radiation or absorption lengths of the crystal for the EMS initiated by electrons or photons. Solid lines represents the EMS component initiated by electrons and dashed lines for EMS component initiated by photons. ( $\bullet$ ) - photon component of EMS, ( $\blacksquare$ ) - electron component of EMS.

The energy carried by the photon component of EMS (initiated by electrons) reaches its maximum value at  $2 L_R$  for silicon and  $1.6 L_R$  for germanium crystals. While the photon numbers reach the maximum at  $3.5 L_R$  for silicon and  $3.2 L_R$  for germanium crystals. The energy carried by electrons is smoothly decreasing for both crystals. The number of electrons reach its maximum

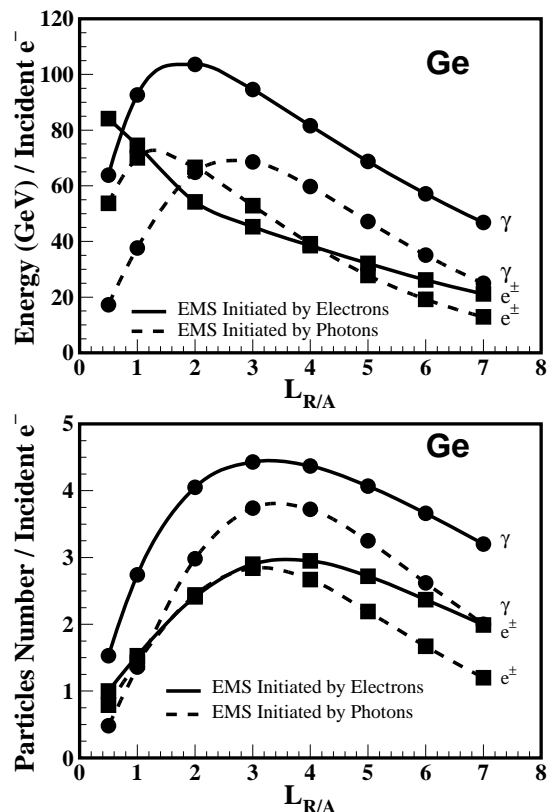


FIG. 4: The energy (top) and number of particles (bottom) of EMS as a function of thickness of an aligned germanium single crystal. The notations are the same as for Fig. 3.

value at  $3.5 L_R$  for silicon crystal and for germanium crystal at  $4.2 L_R$ . The photon and electron components of EMS carry  $\sim 60\%$  and  $\sim 30\%$  of energy of initial electron, respectively, for both crystals. The energy carried by the photon component of EMS are larger than the energy of electrons as seen from the figures.

This is true for number of photons as well, which is about 2 times larger than the number of electrons. This is explained by the CB mechanism of radiation. Initial electrons lose large amount of energy around 100 GeV due to the CB radiation and produce high energy photons as seen from Fig. 5. Simulated photon (top) and electron (bottom) spectra,  $E d^2 N / dE dL_R$ , per unit of radiation length for a silicon crystal are shown. The solid lines represent the spectra from aligned crystal and the dashed lines for unaligned crystal acted as an amorphous. The photon spectrum for ICB smoothly decreases with increasing photon energy. One can observe an expressed photon peak in the vicinity of 100 GeV in case of CB spectrum. The initial electron loses energy mainly for producing high energy photons. Thus, the huge amount of energy is concentrated in the high energy region of the photon spectrum. This concentration of energy leads to the "delay" of EMS development. For example, the amorphous matter or crystal oriented in channeling settings split the energy of electrons very effectively and

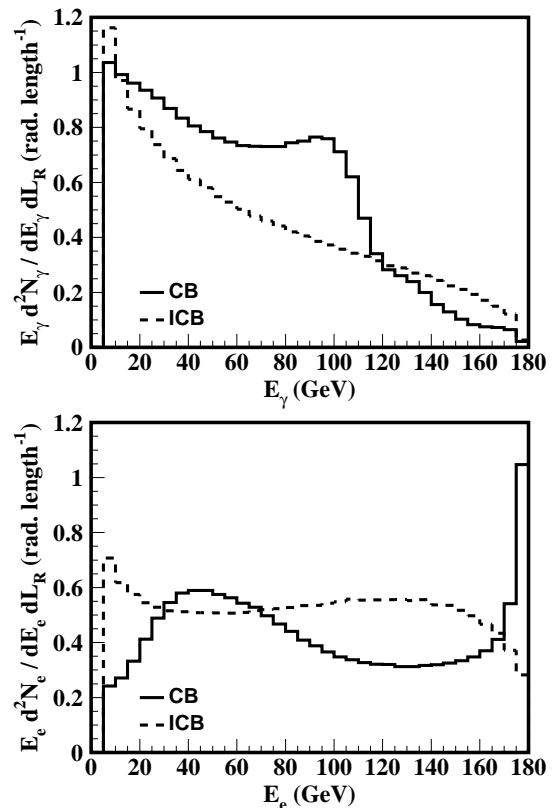


FIG. 5: Simulated photon (top) and electron (bottom) spectra, per unit of radiation length for a silicon crystal. The solid curves represent the spectra from aligned crystal and the dashed curves for unaligned crystal acted as amorphous.

EMS develops more intensively [6].

The energy carried by the electron component of EMS (initiated by photons) reaches its maximum value at  $\sim 1.5 L_A$  for both crystals as seen from the Fig. 3 and Fig. 4. The number of electrons reaches the maximum value at  $\sim 3. L_A$ . The energy carried by the photon component of EMS are approximately the same as energy of electrons at their maximum values. But the number of photons is about 60% larger than number of electrons at  $L_A > 3$ . The behavior of the EMS initiated by photons is approximately the same as in the case of EMS initiated by electrons. The large number of electron-positron pairs are produced in the vicinity of 90 GeV due to the CPP.

## V. CONCLUSION

The computer package presented in this paper is intended for Monte Carlo simulation of the electron and photon beams propagation through the oriented single crystals and amorphous media at high energies. The agreement between the simulation results and measurements is seen to be satisfactory. After finishing the program, the following parameters of the photons and electrons are reported: energy, angular and spatial distribu-

tions and polarization of passed electrons and photons. The important step in the code is the simulation of the photon radiation and  $e^+e^-$  pair production angles, which strongly depends on the initial particles energy. This feature of the computer code can be used for simulation of the photon beam collimation.

The longitudinal behavior of electron and photon induced EMS in single crystals oriented in CB and CPP mode in the energy range between 5 GeV and 175 GeV was investigated. The interesting results are obtained concerning EMS development in single crystals aligned in CB or CPP mode. The crystal does not split the energy of particles as amorphous media. It concentrates the

energy of radiation and produced  $e^+e^-$  pairs in the high energy region after the first interaction act. The crystals behave as a capacitor of energy up to a thickness of  $\sim 2L_{R/A}$ . As a result, the "delayed" EMS take place in the crystal.

### Acknowledgments

The author gratefully acknowledges Prof. M. Velasco (Northwestern University) for a number of very fruitful discussions.

- 
- [1] M. L. Ter-Mikaelian, *High Energy Electromagnetic Processes in Condensed Media* (Wiley Interscience, New-York, 1972).
- [2] A. Apyan et al., Nucl. Instrum. Methods Phys. Res. B **234**, 128 (2005).
- [3] A. Apyan et al., hep-ex/0306028.
- [4] T. M. Jenkins, W. R. Nelson, and A. Rindi, *Monte Carlo Transport of Electrons and Photons* (Plenum Press, New-York, 1988).
- [5] A. Baurichter et al., Nucl. Instrum. Methods Phys. Res. B **152**, 472 (1999).
- [6] V. A. Baskov, V. A. Khablo, V. V. Kim, V. I. Sergienko, B. I. Luchkov, and V. Y. Tugaenko, Nucl. Instrum. Methods Phys. Res. B **122**, 194 (1997).
- [7] P. A. Doyle and P. S. Turner, Acta. Crystallogr., Sect. A **24**, 390 (1968).
- [8] H. Olsen and L. C. Maximon, Phys. Rev. **114**, 887 (1959).
- [9] J. A. Wheeler and E. Lamb, Phys. Rev. **55**, 858 (1939).
- [10] V. N. Baier, V. M. Katkov, and V. M. Strakhovenko, *Electromagnetic Processes at High Energies in Oriented Single Crystals* (World Scientific, Singapore, 1998).
- [11] S. M. Darbinian and N. L. Ter-Isaakian, Nucl. Instrum. Methods Phys. Res. B **187**, 302 (2002).
- [12] R. L. Morin, *Monte Carlo Simulation in the Radiological Sciences* (CRC Press, Boca Raton, Florida, 1988).
- [13] N. Z. Akopov, A. B. Apyan, R. O. Avakian, R. Carrigan, S. M. Darbinian, K. A. Ispirian, Y. V. Kononets, and S. Taroyan, Nucl. Instrum. Methods Phys. Res. B **115**, 372 (1996).
- [14] A. O. Aganians et al., Nucl. Instrum. Methods Phys. Res. B **171**, 577 (2000).
- [15] V. Ghazikhanian et al., sLAC Proposal E-159/160/161 (2000).
- [16] A. Apyan et al., hep-ex/0306041.
- [17] A. Apyan et al., hep-ex/0406026.
- [18] G. Unel et al., Int. J. Mod. Phys. A Suppl. 1C **16**, 1071 (2001).